

# The Reaction $\text{CH}_3 + \text{NO} \rightarrow \text{HCN} + \text{H}_2\text{O}$ . Experimental and Modeling Study

Assa Lifshitz\* and Carmen Tamburu

Department of Physical Chemistry, The Hebrew University, Jerusalem 91904, Israel

Peter Frank and Thomas Just

DLR-Institut für Physikalische Chemie der Verbrennung, Pfaffenwaldring 38, 7000 Stuttgart 80, Germany

Received: June 29, 1992; In Final Form: January 7, 1993

The reaction  $\text{CH}_3 + \text{NO} \rightarrow \text{HCN} + \text{H}_2\text{O}$  was studied behind reflected shocks in a single pulse shock tube by heating mixtures of ethane and nitric oxide and determining the extent of HCN production. The temperature range covered in this investigation was 1100–1330 K at overall densities of approximately  $3 \times 10^{-5} \text{ mol/cm}^3$ . The postshock mixtures contained in addition to hydrogen cyanide minute quantities of  $\text{C}_1$  and  $\text{C}_2$  nitriles and stable products resulting from the decomposition of ethane. These were, in order of decreasing abundance,  $\text{C}_2\text{H}_4$ ,  $\text{CH}_4$ , and  $\text{C}_2\text{H}_2$ . Profiles of mole percent vs reciprocal temperature of the species HCN,  $\text{CH}_4$ ,  $\text{C}_2\text{H}_2$ , and  $\text{C}_2\text{H}_4$  were modeled with a reaction scheme consisting of 18 species and 31 elementary reactions. From these model calculations a rate expression,  $k_1 = 10^{11.8} \exp(-15.0 \times 10^3/RT) \text{ cm}^3 \text{ mol}^{-1} \text{ s}^{-1}$ , is evaluated for the reaction  $\text{CH}_3 + \text{NO} \rightarrow \text{HCN} + \text{H}_2\text{O}$  where  $R$  is expressed in units of  $\text{cal}/(\text{K mol})$ . This reaction is composed of a sequence of reactions, the first one of which is  $\text{CH}_3 + \text{NO} \rightleftharpoons \text{CH}_3\text{NO}$ . Since the latter reaches a state of equilibrium at the very early stages of the reaction, it is suggested that  $k_1$  is equal to  $k_{1b} \times K_{1a}$ , where  $k_{1b}$  is the rate constant for the reaction  $\text{CH}_3\text{NO} (\rightarrow \text{CH}_2=\text{NH} \rightarrow \text{O} \rightarrow \text{CH}_2=\text{N}-\text{OH}) \rightarrow \text{HCN} + \text{H}_2\text{O}$  and  $K_{1a}$  is the equilibrium constant ( $K_c$ ) for the reaction  $\text{CH}_3 + \text{NO} \rightleftharpoons \text{CH}_3\text{NO}$ . The value for  $k_{1b}$  is  $k_{1b} = 10^{13.5} \exp(-50 \times 10^3/RT) \text{ cm}^3 \text{ mol}^{-1} \text{ s}^{-1}$ .

## Introduction

Methyl radicals are important intermediates in the combustion of hydrocarbon fuels. Nitric oxide is formed in flames from either fuel bound nitrogen or atmospheric nitrogen. The reaction between methyl radicals and nitric oxide may therefore play an important role in a large variety of technical combustion processes.

It has been suggested in numerous studies in the past<sup>1-4</sup> that the formation of hydrogen cyanide in fuel nitrogen flames may result from a reaction between methyl radicals and nitric oxide. In a review article on the kinetics of production of HCN in combustion<sup>2</sup> Guibet and Van Tiggelen suggested that the formation of hydrogen cyanide from methyl radicals and nitric oxide proceeds through the following sequence of reactions:



On the other hand, in an article discussing the reactions of methyl radicals with oxygen and nitric oxide,<sup>5</sup> Baldwin and Golden concluded that these reactions were unimportant even at the high temperatures which are of interest in combustion systems.

Whereas the first step in the sequence suggested by Guibet and Van Tiggelen, namely, the recombination of methyl radicals with nitric oxide to form nitrosomethane, has been investigated in the past,<sup>6</sup> there is up to the present date no experimental evidence that hydrogen cyanide is indeed formed according to this mechanism.

Wolff and Wagner<sup>7</sup> have recently investigated the reaction between methyl radicals and nitric oxide behind incident shock waves at temperatures ranging from 1800 to 2150 K. The disappearance of  $\text{CH}_3$  was monitored by UV absorption. They found for the overall rate of the reaction  $\text{CH}_3 + \text{NO} \rightarrow$  products a rate constant of  $2 \times 10^{10} \text{ cm}^3 \text{ mol}^{-1} \text{ s}^{-1}$  at temperatures around 1900 K and estimated from this an activation energy of  $\sim 85 \text{ kJ/mol}$ . The authors could not establish whether hydrogen cyanide or any other product was produced in the reaction.

There have been a number of ab initio calculations of the possible reaction channels leading to the production of hydrogen cyanide from methyl radicals and nitric oxide. Radom et al.<sup>8</sup>

evaluated the energy diagram for the double 1,2 hydrogen shift to form formaldonitrone ( $\text{CH}_2=\text{NH} \rightarrow \text{O}$ ) followed by anti-formaldoxime ( $\text{CH}=\text{N}-\text{OH}$ ), and for the single 1,3 shift to form the syn-formaldoxime, followed by syn  $\rightarrow$  anti isomerization. The calculations show that the 1,3 hydrogen shift had a slightly higher barrier than the two 1,2 successive shifts. Similar calculations were carried out by Melius<sup>9</sup> who evaluated also the energy barrier for the formation of hydrogen cyanide and water from anti-formaldoxime. Saito et al.<sup>10</sup> studied the thermal decomposition of formaloxime to  $\text{H}_2\text{O}$  and HCN by monitoring the UV absorption of the reactant and the IR emission of HCN. They have also carried out detailed ab initio calculations of the transition structure for this decomposition and found a very good agreement between the calculated and the measured rate constant.

The present article describes a first attempt to identify HCN in the reaction between methyl radicals and nitric oxide and to determine the rate constant for its formation.

## Experimental Section

**Apparatus.** The reaction between ethane and nitric oxide was studied behind reflected shocks in a pressurized driver, 52-mm-i.d. single pulse shock tube made of stainless steel tubing. The tube and its mode of operation have been described in a previous publication<sup>11</sup> and will be reported here only very briefly. The driven section was 4 m long and was divided in the middle by a 52-mm ball valve. The driver had a variable length up to a maximum of 2.7 m and could be varied in 1-in. steps in order to obtain the best cooling conditions. Sections of the shock tube were connected with copper gaskets, except for the last half of the driven section which used gold gaskets to ensure smoothness in the region of the well formed shock flow. A 36-L dump tank was connected to the driven section near the diaphragm holder to prevent reflection of transmitted shocks and to reduce the final pressure in the tube. The driven section was separated from the driver by a "Mylar" polyester film of thickness depending upon the desired shock strength.

After the tube was pumped down to approximately  $10^{-5}$  Torr, the reaction mixture was introduced into the section between the

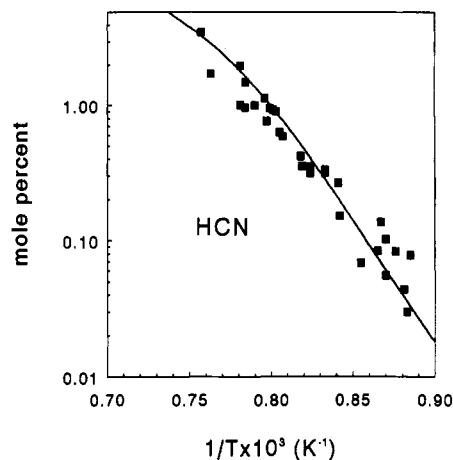


**Figure 1.** Mole percent of HCN as a function of reciprocal temperature. The squares are the experimental points, and the solid line is the calculated profile. The agreement is very good.

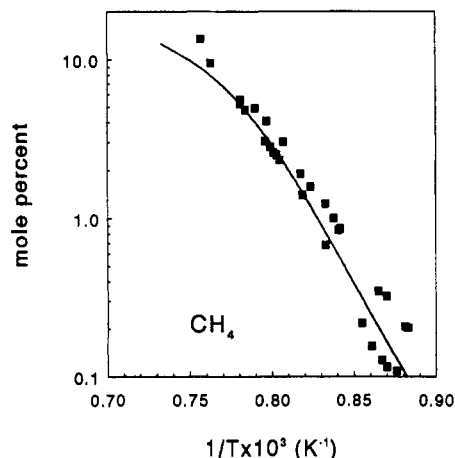


**Figure 2.** Mole percent of CH<sub>4</sub> as a function of reciprocal temperature. The squares are the experimental points, and the solid line is the calculated profile.

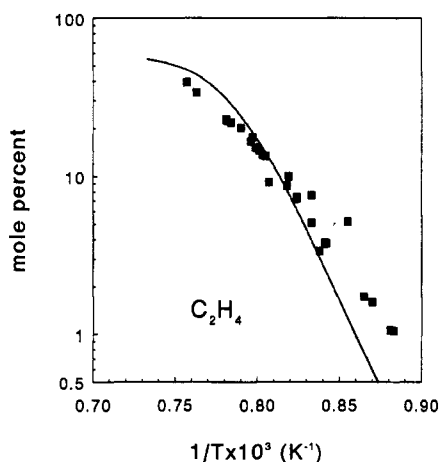


**Figure 3.** Mole percent of C<sub>2</sub>H<sub>4</sub> as a function of reciprocal temperature. The squares are the experimental points, and the solid line is the calculated profile.

ball valve and the end plate and pure argon into the section between the diaphragm and the valve, including the dump tank. After the shock was fired, gas samples were taken from the tube through an outlet in the driven section near the end plate and were analyzed on a Hewlett-Packard Model 5890A gas chromatograph using flame ionization (FID) and nitrogen phosphorous (NPD) detectors.

**Reflected Shock Temperatures and Densities.** Reflected shock temperatures were evaluated from the extent of decomposition

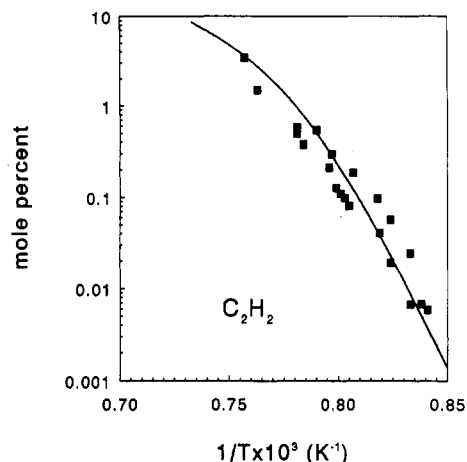


**Figure 4.** Mole percent of C<sub>2</sub>H<sub>2</sub> as a function of reciprocal temperature. The squares are the experimental points, and the solid line is the calculated profile.

of 1,1,1-trifluoroethane to 1,1-difluoroethylene and hydrogen fluoride, an internal standard which served as a chemical thermometer in this investigation. The decomposition of 1,1,1-trifluoroethane is a clean unimolecular reaction which proceeds with a preexponential factor of  $A = 10^{14.51} \text{ s}^{-1}$  and an activation energy of  $E = 72.75 \text{ kcal/mol}$ .<sup>12</sup> The reflected shock temperatures were calculated from the following equation:

$$T = -(E/R) / \ln \left\{ -\frac{1}{At} \ln(1 - \chi) \right\} \quad (\text{I})$$

where  $t$  is the reaction dwell time and  $\chi$  is the extent of decomposition defined as

$$\chi = [\text{CH}_2\text{CF}_2]_t / ([\text{CH}_2\text{CF}_2]_t + [\text{CH}_3\text{CF}_3]_t) \quad (\text{II})$$

Reflected shock densities were calculated from the measured incident shock velocities using the three conservation equations and the ideal gas equation of state. The velocities were measured with two high frequency pressure transducers placed 300 mm apart near the end plate of the driven section. A third transducer placed at the center of the end plate provided measurements of the reaction dwell times (about 2 ms) with an accuracy of approximately 5%. Cooling rates were approximately  $5 \times 10^5 \text{ K/s}$ .

**Materials and Analysis.** Reaction mixtures containing 0.25% 1,1,1-trifluoroethane, 1% ethane, and 10% nitric oxide in argon were prepared and stored at high pressures in stainless steel cylinders. Both the cylinders and the line were pumped down to better than  $10^{-5}$  Torr before the preparation of the mixtures.

The nitric oxide was CP grade listed as 99% pure. A mass spectrometric analysis showed  $\sim 0.4\%$  nitrous oxide in the nitric oxide. The ethane used was research grade listed as 99.96% pure. 1,1,1-Trifluoroethane (unlisted purity) was obtained from PCR. Neither 1,1-difluoroethylene nor other fluorocarbon impurities could be detected in the unshocked samples. Argon was UHP grade listed as 99.9995%, and helium was 99.999% pure. All the gases were obtained from the Matheson Gas Co. and were used without further purification.

Gas analyses were performed in the following manner: post shock samples were injected into the gas chromatograph (HP Model 5890A) and were then equally divided between two 2-m Porapak N columns connected to FID and NPD detectors, respectively. The Porapak N column which was connected to a FID separated and quantitatively determined the hydrocarbons in the samples. The second column connected to the NPD determined the HCN. A standard mixture containing C<sub>2</sub>H<sub>6</sub> and HCN at a ratio of  $\sim 10:1$  was run on the two columns in order to determine sensitivity ratios in the two detectors and thus combine the results obtained from the two columns. This

TABLE I: Experimental Conditions and Postshock Product Distribution

$T_5$ (K)	$C_5 \times 10^5$ (mol/cm <sup>3</sup> )	dwell time (ms)	product distribution (%)				
			$\text{C}_2\text{H}_6$	$\text{CH}_4$	$\text{C}_2\text{H}_4$	$\text{C}_2\text{H}_2$	HCN
1133	3.52	2.08	98.71	0.203	1.05		0.030
1135	3.17	1.95	98.68	0.207	1.07		0.044
1150	3.43	1.84	98.03	0.322	1.59		0.056
1156	3.35	2.00	97.84	0.347	1.73		0.084
1169	3.41	1.75	94.51	0.218	5.19	0.0086	0.068
1187	2.97	2.03	95.21	0.860	3.78		0.152
1189	3.17	1.94	95.04	0.843	3.84	0.0058	0.266
1194	2.92	2.07	95.60	1.00	3.39	0.0068	
1201	3.00	2.08	93.31	1.23	5.12	0.0067	0.333
1201	3.00	1.97	91.35	0.679	7.63	0.023	0.318
1213	3.18	1.80	90.82	1.58	7.23	0.019	0.353
1214	2.99	1.97	90.62	1.57	7.43	0.057	0.317
1221	2.95	1.86	88.20	1.39	10.01	0.041	0.354
1222	2.83	1.94	88.84	1.89	8.75	0.097	0.421
1239	2.78	2.01	86.96	3.03	9.23	0.185	0.591
1242	3.05	1.91	83.49	2.32	13.48	0.080	0.631
1245	3.03	2.05	82.83	2.49	13.68	0.098	0.903
1249	2.70	2.17	81.80	2.58	14.58	0.109	0.931
1252	3.00	1.86	80.87	2.81	15.24	0.126	0.956
1255	2.83	1.76	77.22	4.07	17.65	0.295	0.765
1257	2.78	2.00	79.01	3.04	16.61	0.212	1.13
1266	2.72	1.91	73.29	4.92	20.24	0.542	1.00
1275	2.77	2.00	72.03	4.78	21.84	0.379	0.966
1275	2.77	2.00	71.57	4.81	21.75	0.377	1.49
1280	2.87	1.86	69.39	5.57	22.47	0.582	1.98
1280	2.74	1.93	70.33	5.22	22.94	0.496	1.01
1310	2.82	1.76	53.51	9.51	33.77	1.49	1.72
1321	3.61	1.95	40.24	13.47	39.33	3.43	3.53

procedure was repeated periodically after every few analyses in order to prevent errors resulting from variation in the sensitivity of one detector relative to the other.

Areas under the GC peaks were integrated by a Spectra Physics Model SP4200 computing integrator. The information accumulated on the integrator was transferred to an IBM/PC for data reduction and graphical presentation.

**Evaluation of Product Concentrations.** Product concentrations were evaluated from their GC peak areas in the following manner:

(1) The concentration of ethane behind the reflected shock prior to decomposition,  $C_5(\text{ethane})_0$ , is given by

$$C_5(\text{ethane})_0 = \{p_1(\%(\text{ethane}))\rho_5/\rho_1\}/100RT_1 \quad (\text{III})$$

where  $p_1$  is the pressure in the tube prior to shock heating,  $\%(\text{ethane})$  is the percent of ethane in the original mixture,  $\rho_5/\rho_1$  is the compression behind the reflected shock, and  $T_1$  is room temperature.

(2) Assuming carbon atom balance, the concentration of ethane behind the reflected shock prior to decomposition in terms of its peak area,  $A(\text{ethane})_0$  is given by

$$A(\text{ethane})_0 = A(\text{ethane})_i + \frac{1}{2} \sum N(pr_i) A(pr_i)_i / S(pr_i) \quad (\text{IV})$$

where  $A(\text{ethane})_i$  is the peak area of ethane in the shocked sample,  $A(pr_i)_i$  is the peak area of a product  $i$  in the shocked sample,  $S(pr_i)$  is its sensitivity relative to ethane, and  $N(pr_i)$  is the number of its carbon atoms.

(3) The concentration of a product  $i$  in the shocked sample is given by

$$C_5(pr_i) = A(pr_i)_i / S(pr_i) \{C_5(\text{ethane})_0 / A(\text{ethane})_0\} \quad (\text{V})$$

Since  $A(\text{ethane})_0$  is not available in the postshock analysis, its value is calculated from eq II.

## Results and Discussion

**Product Distribution.** In order to identify the quantitatively determine the reaction products obtained in postshock mixtures of ethane and nitric oxide, some 30 tests were run with mixtures

containing 0.25% 1,1,1-trifluoroethane, 1% ethane, and 10% nitric oxide in argon, covering the temperature range 1100–1320 K. Over this temperature range the stable products  $\text{C}_2\text{H}_4$ ,  $\text{CH}_4$ ,  $\text{C}_2\text{H}_2$ , and HCN were found. Details of the experimental conditions and the distribution of products are given in Table I. The table shows the temperature behind the reflected shock  $T_5$  as calculated from the conversion of the internal standard, the overall density behind the reflected shock  $C_5$ , the dwell times, the mole percent of ethane, and the various products in the mixture as obtained in the postshock analyses. The percent of a given product in the total sample, as shown in the table, corresponds to its mole percent,  $(100C_i/\sum C_i)$  irrespective of the number of its carbon atoms and not including nitric oxide and argon. Figures 1–4 show the temperature profiles of these four products plotted as mole percent vs reciprocal temperature. The solid squares are the experimental points, and the lines are the profiles calculated with the reaction scheme shown in Table II.

A ratio of 1:10 ethane to nitric oxide was chosen in these experiments in order to suppress subsequent reactions of methyl and ethyl radicals with hydrogen cyanide and thus simplify the reaction scheme. Under these conditions and over the temperature range covered in this investigation, very small amounts of propylene ( $\text{C}_3\text{H}_6$ ), acetonitrile ( $\text{CH}_3\text{CN}$ ), and propionitrile ( $\text{C}_2\text{H}_5\text{CN}$ ) were found in the postshock mixtures, particularly at high temperatures. Their production was not included as part of the reaction scheme.

**Reaction Scheme and Computer Modeling.** Since the production of hydrogen cyanide by a reaction of methyl radicals with nitric oxide is not the only reaction in the system, the evaluation of its rate constant requires a complete modeling study. Its rate parameters must be determined by a best fit to the experimental mole percent of HCN. Since several other products, such as ethylene, methane, and acetylene, are obtained in the process (some at even higher concentrations than HCN), the computer modeling must also reproduce their mole percent. In this way the uncertainty in determining the rate constant for the production of HCN is considerably decreased.

In order to account quantitatively for the product distribution and its temperature dependence, a reaction scheme consisting of

TABLE II: Reaction Scheme for the C<sub>2</sub>H<sub>6</sub> + NO System

reaction	A	n	E	k <sub>r</sub> (1250 K)	k <sub>r</sub> (1250 K)	ΔH <sup>o</sup>	source
1. CH <sub>3</sub> + NO → HCN + H <sub>2</sub> O	6.3 × 10 <sup>11</sup>	0	15.0	1.48 × 10 <sup>9</sup>	2.25 × 10 <sup>-5</sup>	-82.9	a
2. CH <sub>3</sub> + NO → OH + CH <sub>2</sub> N	1.00 × 10 <sup>12</sup>	0	21.7	1.58 × 10 <sup>8</sup>	5.43 × 10 <sup>9</sup>	12.6	ref 18
3. CH <sub>2</sub> N + Ar → HCN + H + Ar	2.29 × 10 <sup>15</sup>	0	26.7	4.86 × 10 <sup>10</sup>	9.30 × 10 <sup>14</sup>	25.9	estimate
4. C <sub>2</sub> H <sub>6</sub> → CH <sub>3</sub> + CH <sub>3</sub>	1.71 × 10 <sup>16</sup>	0	86.3	1.42 × 10 <sup>1</sup>	1.26 × 10 <sup>13</sup>	90.8	ref 17
5. CH <sub>3</sub> + CH <sub>3</sub> → C <sub>2</sub> H <sub>5</sub> + H	2.80 × 10 <sup>13</sup>	0	13.5	1.22 × 10 <sup>11</sup>	1.81 × 10 <sup>14</sup>	11.6	ref 19
6. C <sub>2</sub> H <sub>6</sub> + CH <sub>3</sub> → C <sub>2</sub> H <sub>5</sub> + CH <sub>4</sub>	5.48 × 10 <sup>-1</sup>	4	8.28	4.77 × 10 <sup>10</sup>	3.21 × 10 <sup>9</sup>	-5.0	ref 15
7. CH <sub>3</sub> + C <sub>2</sub> H <sub>5</sub> → CH <sub>4</sub> + C <sub>2</sub> H <sub>4</sub>	2.00 × 10 <sup>12</sup>	0	0	2.00 × 10 <sup>12</sup>	3.18 × 10 <sup>12</sup>	-69.5	estimate
8. C <sub>2</sub> H <sub>5</sub> → C <sub>2</sub> H <sub>4</sub> + H	2.09 × 10 <sup>11</sup>	0	30.8	8.62 × 10 <sup>5</sup>	2.69 × 10 <sup>12</sup>	38.0	b
9. C <sub>2</sub> H <sub>6</sub> + H → C <sub>2</sub> H <sub>5</sub> + H <sub>2</sub>	1.43 × 10 <sup>14</sup>	0	9.58	3.03 × 10 <sup>12</sup>	8.69 × 10 <sup>9</sup>	-0.38	ref 17
10. C <sub>2</sub> H <sub>4</sub> + Ar → C <sub>2</sub> H <sub>2</sub> + H <sub>2</sub> + Ar	2.11 × 10 <sup>17</sup>	0	78.7	3.67 × 10 <sup>3</sup>	1.91 × 10 <sup>9</sup>	44.3	ref 17
11. C <sub>2</sub> H <sub>4</sub> + H → C <sub>2</sub> H <sub>3</sub> + H <sub>2</sub>	2.04 × 10 <sup>14</sup>	0	14.4	6.31 × 10 <sup>11</sup>	1.53 × 10 <sup>11</sup>	3.60	ref 17
12. C <sub>2</sub> H <sub>4</sub> + CH <sub>3</sub> → C <sub>2</sub> H <sub>3</sub> + CH <sub>4</sub>	3.03 × 10 <sup>13</sup>	0	21.5	5.35 × 10 <sup>9</sup>	3.04 × 10 <sup>10</sup>	2.38	ref 17
13. C <sub>2</sub> H <sub>3</sub> + Ar → C <sub>2</sub> H <sub>2</sub> + H + Ar	8.00 × 10 <sup>14</sup>	0	31.5	2.49 × 10 <sup>9</sup>	5.33 × 10 <sup>15</sup>	40.7	ref 17
14. C <sub>2</sub> H <sub>3</sub> + H → C <sub>2</sub> H <sub>2</sub> + H <sub>2</sub>	9.60 × 10 <sup>13</sup>	0	0	9.60 × 10 <sup>13</sup>	4.48 × 10 <sup>2</sup>	-65.5	ref 17
15. C <sub>2</sub> H <sub>3</sub> + CH <sub>3</sub> → C <sub>2</sub> H <sub>2</sub> + CH <sub>4</sub>	3.90 × 10 <sup>11</sup>	0	0	3.90 × 10 <sup>11</sup>	4.26 × 10 <sup>1</sup>	-66.7	ref 17
16. C <sub>2</sub> H <sub>6</sub> + C <sub>2</sub> H <sub>3</sub> → C <sub>2</sub> H <sub>4</sub> + C <sub>2</sub> H <sub>5</sub>	6.01 × 10 <sup>2</sup>	3.3	10.5	1.46 × 10 <sup>11</sup>	1.72 × 10 <sup>9</sup>	-7.4	ref 15
17. CH <sub>4</sub> + Ar → CH <sub>3</sub> + H + Ar	1.38 × 10 <sup>17</sup>	0	88.7	4.29 × 10 <sup>1</sup>	8.41 × 10 <sup>17</sup>	107.4	ref 17
18. OH + C <sub>2</sub> H <sub>6</sub> → C <sub>2</sub> H <sub>5</sub> + H <sub>2</sub> O	1.71 × 10 <sup>8</sup>	1.59	1.31	8.58 × 10 <sup>12</sup>	2.62 × 10 <sup>8</sup>	-19.0	ref 17
19. OH + C <sub>2</sub> H <sub>4</sub> → C <sub>2</sub> H <sub>3</sub> + H <sub>2</sub> O	1.57 × 10 <sup>4</sup>	2.75	4.17	9.62 × 10 <sup>11</sup>	2.49 × 10 <sup>9</sup>	-11.7	ref 17
20. H + OH + Ar → H <sub>2</sub> O + Ar	2.22 × 10 <sup>22</sup>	-2	0	1.42 × 10 <sup>16</sup>	3.30 × 10 <sup>-4</sup>	-121.5	ref 17
21. H + H + Ar → H <sub>2</sub> + Ar	5.44 × 10 <sup>18</sup>	-1.3	0	5.12 × 10 <sup>14</sup>	1.12 × 10 <sup>-3</sup>	-106.2	ref 17
22. C <sub>2</sub> H <sub>5</sub> + NO → C <sub>2</sub> H <sub>5</sub> NO	8.00 × 10 <sup>12</sup>	0	0	8.00 × 10 <sup>12</sup>	6.84 × 10 <sup>8</sup>	-40.7	estimate
23. C <sub>2</sub> H <sub>5</sub> + NO → C <sub>2</sub> H <sub>4</sub> + HNO	3.00 × 10 <sup>11</sup>	0	10.0	5.36 × 10 <sup>9</sup>	2.15 × 10 <sup>8</sup>	-14.0	estimate
24. C <sub>2</sub> H <sub>3</sub> + NO → C <sub>2</sub> H <sub>2</sub> + HNO	3.00 × 10 <sup>11</sup>	0	10.0	5.36 × 10 <sup>9</sup>	1.47 × 10 <sup>8</sup>	-11.2	estimate
25. HNO + Ar → H + NO + Ar	1.50 × 10 <sup>16</sup>	0	48.7	4.63 × 10 <sup>7</sup>	3.60 × 10 <sup>15</sup>	51.9	ref 20
26. CH <sub>3</sub> + HNO → CH <sub>4</sub> + NO	5.00 × 10 <sup>12</sup>	0	8.0	2.00 × 10 <sup>11</sup>	7.93 × 10 <sup>2</sup>	-55.6	estimate
27. H + HNO → H <sub>2</sub> + NO	1.33 × 10 <sup>12</sup>	0	-2.36	3.45 × 10 <sup>12</sup>	5.86 × 10 <sup>2</sup>	-54.3	ref 17
28. C <sub>2</sub> H <sub>5</sub> + HNO → C <sub>2</sub> H <sub>6</sub> + NO	5.00 × 10 <sup>12</sup>	0	8.0	2.00 × 10 <sup>11</sup>	1.18 × 10 <sup>4</sup>	-50.6	estimate
29. C <sub>2</sub> H <sub>3</sub> + HNO → C <sub>2</sub> H <sub>4</sub> + NO	5.00 × 10 <sup>12</sup>	0	8.0	2.00 × 10 <sup>11</sup>	1.39 × 10 <sup>2</sup>	-58.0	estimate
30. OH + HNO → H <sub>2</sub> O + NO	1.08 × 10 <sup>13</sup>	0	0	1.08 × 10 <sup>13</sup>	1.95 × 10 <sup>1</sup>	-69.6	ref 17
31. HNO + NO → N <sub>2</sub> O + OH	2.00 × 10 <sup>12</sup>	0	26.0	5.70 × 10 <sup>7</sup>	1.46 × 10 <sup>6</sup>	-15.6	ref 20

<sup>a</sup> This investigation. <sup>b</sup> Reference 17 with falloff correction. Reference 17—Best fit to *NIST-Chemical Kinetics Data Base*. ΔH<sub>r</sub><sup>o</sup> are expressed in units of kcal/mol. Rate constants are expressed as  $k = AT^n \exp(-E/RT)$  in units of cm<sup>3</sup> s kcal/mol.

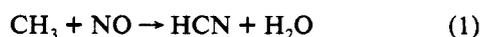
18 species and 31 elementary reactions was constructed. The scheme is listed in Table II. The calculations were performed under the assumption of constant density during a reaction time of 2 ms.

The thermodynamic properties of the species used for calculating the equilibrium constants of the reactions and the temperature change in the course of the reaction were obtained from several sources.<sup>9,13-16</sup> Most of the Arrhenius rate parameters used in these calculations were based on the *NIST-Chemical Kinetic Data Base*<sup>17</sup> and were chosen as the best fit to a large number of entries for each reaction. Some additional sources were also used, particularly when they were absent from the *NIST-Chemical Kinetic Data Base*. The suggested rate parameters for reaction 1 are the outcome of this investigation. The sources for the rate constants are listed in column 7 of Table II.

Figures 1-4 show comparisons between the experimental and the calculated mole percent of four products based on the reaction scheme listed in Table II. The squares are the experimental points, and the solid lines are the calculated profiles. The agreement seems to be satisfactory and can serve as a basis for evaluating the rate parameters for reaction 1.

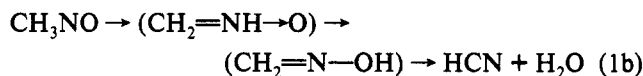
Owing to the endothermicity of the global reaction, there is a temperature drop during the course of the reaction. It is approximately 2 K at 1175 K and 42 K at the upper end of the temperature range, 1330 K. Since we used a chemical thermometer to evaluate the reflected shock temperatures, they correspond to the average of the initial and the final temperatures. The calculated mole percents shown in Figures 1-4 which correspond to initial temperatures of 1100, 1175, 1250, and 1330 K are thus plotted against the reciprocal of 1100, 1174, 1244, and 1309, respectively.

The rate expression suggested for the reaction



is  $k_1 = 10^{11.8} \exp(-15.0 \times 10^3/RT) \text{ cm}^3 \text{ mol}^{-1} \text{ s}^{-1}$ , where  $R$  is expressed in units of cal/(K mol).

Reaction 1 is, in fact, not an elementary reaction since it proceeds via a sequence of intermediates, the first one of which is nitrosomethane.



Let us now evaluate the rate expression for the unimolecular isomerization and decomposition of nitrosomethane. We will assume that the isomerization step is rate determining as it seems to have the highest barrier.<sup>18</sup>

Assuming a steady-state concentration for CH<sub>3</sub>NO, the rate of HCN formation is given by

$$d[\text{HCN}]/dt = k(f)_{1a}k_{1b}[\text{CH}_3][\text{NO}]/(k(r)_{1a} + k_{1b}) \quad (VI)$$

where  $k(r)_{1a} = k(f)_{1a}/K_{1a}$ . Since the exit channel of nitrosomethane to formaldonitrone is by more than 10 kcal/mol<sup>9,13</sup> above its exit channel to CH<sub>3</sub> + NO, it is reasonable to assume that  $k(r)_{1a} \gg k(f)_{1b}$ . The experimental first-order rate constant for the formation of HCN,  $k_1$ , is thus given by  $K_{1a}k_{1b}$ .

The equilibrium constant of reaction 1a,  $K_{1a}$ , is given by  $K_{1a} = \exp\{-\Delta H_r^\circ/RT + \Delta S_r^\circ/R\}RT$ . With ΔH<sub>r</sub><sup>o</sup>(1a) = -37.6 kcal/mol and ΔS<sub>r</sub><sup>o</sup>(1a) = -32.7 cal/(K mol),  $K_{1a}$  can be expressed as  $K_{1a} = 1.98 \times 10^{-2} \exp(35140/RT) \text{ cm}^3 \text{ mol}^{-1}$ . This gives for  $k_{1b}$  the value of  $3.2 \times 10^{13} \exp(-50 \times 10^3/RT) \text{ s}^{-1}$ .

Owing to contributions from the temperature dependence of the preexponential factor, the activation energy of 50 kcal/mol is about 3 kcal/mol higher than the true reaction barrier. The main contribution comes from the term  $kT/h$  in the rate constant which adds a value of  $RT$  to the barrier.  $\{\partial \ln T/\partial(1/T) = T\}$ . This around 1250 K is 2.5 kcal/mol. Our evaluated barrier for the nitrosomethane-formaldonitrone isomerization is thus 47 kcal/mol, which is identical with a barrier height of 47 kcal/mol

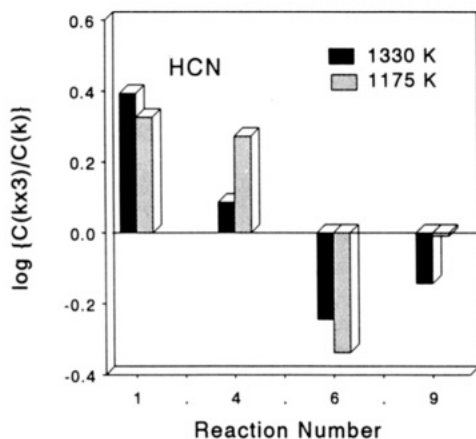


**Figure 5.** Sensitivity spectrum of HCN production, at 1175 and 1330 K. It gives the percent change in the concentration of HCN resulting from a factor of 3 increase in the rate constants. Only reactions that show an effect of at least 25% at one of the two temperatures are considered. The production rate of HCN is sensitive mostly to reaction 1 and less to the production rate of methyl radicals.

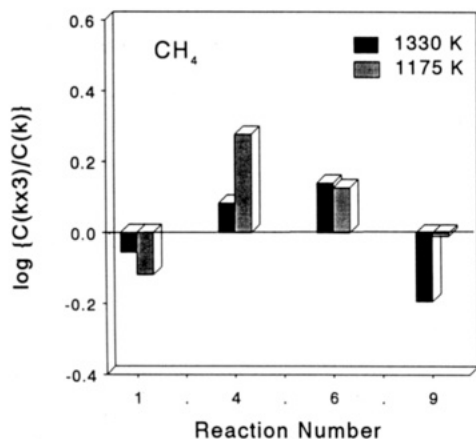


**Figure 6.** Sensitivity spectrum of  $\text{CH}_4$  production at 1175 and 1330 K. It gives the percent change in the concentration of  $\text{CH}_4$  resulting from a factor of 3 increase in the rate constants. Only reactions that show an effect of at least 25% at one of the two temperatures are considered.

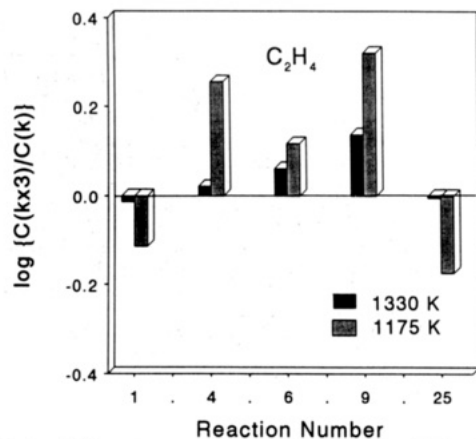


**Figure 7.** Sensitivity spectrum of  $\text{C}_2\text{H}_4$  production at 1175 and 1330 K. It gives the percent change in the concentration of  $\text{C}_2\text{H}_4$  resulting from a factor of 3 increase in the rate constants. Only reactions that show an effect of at least 25% at one of the two temperatures are considered.

calculated by Melius.<sup>9</sup> The preexponential factor of  $3.2 \times 10^{13} \text{ s}^{-1}$  is also in reasonable accord with an isomerization involving 1,2 hydrogen shifts.

**Sensitivity Analysis.** Figures 5–8 show sensitivity analyses for the formation of the four products HCN,  $\text{CH}_4$ ,  $\text{C}_2\text{H}_4$ , and  $\text{C}_2\text{H}_2$  calculated at 1175 and 1330 K, respectively. They show, on a logarithmic scale, the change in the concentration of a given product, for a reaction time of 2 ms, due to a factor of 3 increase

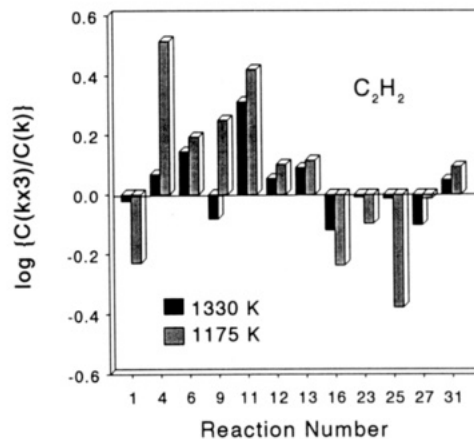


**Figure 8.** Sensitivity spectrum of  $\text{C}_2\text{H}_2$  production at 1175 and 1330 K. It gives the percent change in the concentration of  $\text{C}_2\text{H}_2$  resulting from a factor of 3 increase in the rate constants. Only reactions that show an effect of at least 25% at one of the two temperatures are considered. The production rate of  $\text{C}_2\text{H}_2$  is sensitive to the reactions which are associated with hydrogen atoms.

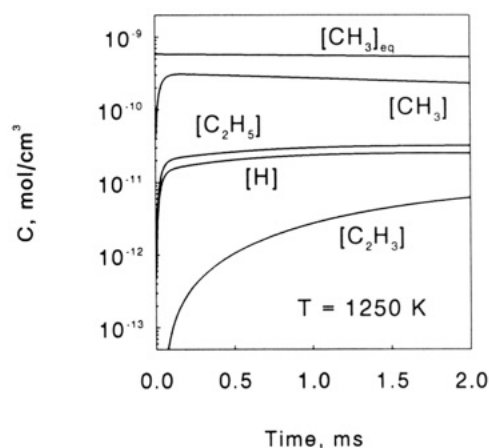


**Figure 9.** Time dependent concentrations of the four free radicals that are active in the system. Except for  $\text{C}_2\text{H}_3$  they all reach a steady-state concentration at the early stages of the reactions. The steady-state concentration of  $\text{CH}_3$  is only mildly below its equilibrium concentration.

in the forward (and reverse) rate constants. The figures concentrate on reactions that have the most influence on the production rates of these species (at least an effect of 25% at either 1175 or 1330).

These four figures show that although the HCN and the hydrocarbon systems are coupled, the production rate of HCN is still most sensitive to reaction 1, whereas the sensitivity of the hydrocarbon production to this reaction is much smaller. The small sensitivity that can still be seen is owing to the competition for methyl radicals by ethane and ethylene and by NO. As can be seen in Figure 5, the reactions in the hydrocarbon system to which the production rate of HCN is most sensitive are the production of methyl radicals by the dissociation of ethane (reaction 4) and the depletion of methyl radicals by reaction with ethane (reaction 6). In fact, one would have expected a much higher sensitivity to reaction 4 since the production rate of HCN is directly proportional to the concentration of  $\text{CH}_3$  radicals in the system. However, the concentration of methyl radicals, which reach a steady-state concentration at the very early stages of the reaction, is not much below their equilibrium concentration (Figure 9). Thus, changing the rate of reaction 4 has a relatively mild effect on the concentration of methyl radicals and thus on the production rate of HCN. The deviation of the steady-state concentration of methyl radicals from their equilibrium concentration diminishes at high temperatures and so is the sensitivity of HCN production to reaction 4 (Figure 5). Owing to the coupling between the HCN and the hydrocarbon system, the

uncertainty in the rates of reactions 4 and 6 is transferred to the rate of reaction 1. However, since the sensitivity is not very high, and the  $\text{CH}_3$  system is known with relatively high accuracy, it has a minimal effect on the evaluation of  $k_1$ .

As can be seen in Figure 8, the production rate of acetylene is sensitive to a large number of reactions, most of which are associated with H atom and  $\text{C}_2\text{H}_5$  radical reactions. H atoms produce  $\text{C}_2\text{H}_3$  radicals, the dissociation of which produces  $\text{C}_2\text{H}_2$ . It should be mentioned here that reaction 25 proceeds in a direction opposite to its listing in Table II. Its negative effect on acetylene production is due to the reaction of H atoms with NO. The sensitivity spectrum of the other two hydrocarbons is self-evident. In most cases the sensitivity at high temperatures is smaller than the one at low temperatures, mainly because the system slows down owing to the high conversion of the reactant.

The best fit for the mole percent of HCN that is obtained by the reaction scheme is not very sensitive to the precise choice of  $E_1$  and  $A_1$  as long as the *absolute* value of  $k_1$  in the middle of the temperature range (1250 K) remains the same. A variation of  $E_1$  by 3 kcal/mol, for example, when compensated by an equivalent variation in  $A_1$  impairs the fit only very slightly. The suggested values of  $A_1$  and  $E_1$  had to be based, therefore, on additional analysis as follows:

(1) A value of  $A_1 = 6.3 \times 10^{11} \text{ cm}^3 \text{ mol}^{-1} \text{ s}^{-1}$  leads to a value of  $3.2 \times 10^{13} \text{ s}^{-1}$  for  $\text{CH}_3\text{NO}$  isomerization. This value is in reasonable agreement with 1,2 hydrogen shifts as rate determining.

(2) The value of  $E_1 = 15 \text{ kcal/mol}$  leads to  $\sim 50 \text{ kcal/mol}$  for the activation energy of the isomerization. This value is in excellent agreement with an isomerization barrier of 47 kcal/mol calculated by Melius.<sup>9</sup>

(3) Hoffmann et al.<sup>18</sup> have estimated at 2000 K a ratio of 0.4:1 for the relative contribution of the  $\text{CH}_3 + \text{NO} \rightarrow \text{CH}_2\text{N} + \text{OH}$  channel to the total rate of the reaction of  $\text{CH}_3 + \text{NO}$ . When our rate constant  $k_1$  is extrapolated to 2000 K, a ratio of  $\sim 0.3:1$  is obtained. On the assumption that the channel  $\text{CH}_3 + \text{NO} \rightarrow \text{HCN} + \text{H}_2\text{O}$  is the major channel for the  $\text{CH}_3 + \text{NO}$  reaction, these two values are in very good agreement.

Figure 10 shows an Arrhenius extrapolation of  $k_1$  to higher temperatures where data on the overall reaction of methyl radicals with  $\text{NO}$ <sup>7</sup> and the channel  $\text{CH}_3 + \text{NO} \rightarrow \text{CH}_2\text{N} + \text{OH}$ <sup>18</sup> are available. According to these data the rates of channels 1 and 2 together are very close to the total  $\text{CH}_3 + \text{NO}$  reaction.

## Conclusion

The production of HCN in a system of ethane and nitric oxide can be simulated with a reaction scheme containing 18 species and 31 elementary reactions. A rate expression  $k_1 = 10^{11.8} \exp(-15.0 \times 10^3/RT) \text{ cm}^3 \text{ mol}^{-1} \text{ s}^{-1}$  for the reaction  $\text{CH}_3 + \text{NO} \rightarrow \text{HCN} + \text{H}_2\text{O}$  is obtained, where  $R$  is expressed in units of cal/(K mol), by fitting calculated to experimental mole percent of HCN. This rate expression extrapolates very well to high temperatures where data on reaction of methyl radicals with NO are available. This value of  $k_1$  leads to a rate expression of  $k_{1b} = 10^{13.5} \exp(-50$

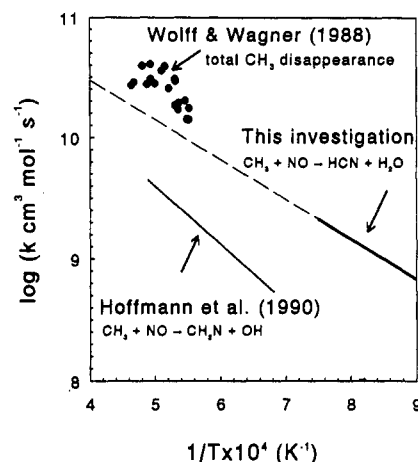


**Figure 10.** Arrhenius extrapolation of the rate constant for the reaction  $\text{CH}_3 + \text{NO} \rightarrow \text{HCN} + \text{H}_2\text{O}$  to higher temperatures. The agreement between the high and the low temperature data is very good.

$\times 10^3/RT \text{ s}^{-1}$  for the reaction  $\text{CH}_3\text{NO} (\rightarrow \text{CH}_2=\text{NH} \rightarrow \text{O} \rightarrow \text{CH}_2=\text{N}-\text{OH}) \rightarrow \text{HCN} + \text{H}_2\text{O}$ .

**Acknowledgment.** This work was supported by a grant from the Volkswagen Foundation.

## References and Notes

- Fenimore, C. P.; Jones, G. W. *J. Phys. Chem.* **1961**, *65*, 1532.
- Guibet, J. C.; Van Tigellen, A. *Rev. Inst. Fr. Pet.* **1963**, *12*, 1284.
- Haynes, B. S. *Combust. Flame* **1977**, *28*, 81.
- Morley, C. *Combust. Flame* **1976**, *27*, 189.
- Baldwin, C. A.; Golden, D. M. *Chem. Phys. Lett.* **1978**, *55*, 359.
- Washida, N. *J. Chem. Phys.* **1980**, *73*, 1665.
- Wolff, Th.; Wagner, H. G. *Ber. Bunsen-Ges. Phys. Chem.* **1988**, *92*, 678.
- Adeney, P. D.; Bouma, W. J.; Radom, L.; Rodwell, W. R. *J. Am. Chem. Soc.* **1980**, *102*, 4069.
- Melius, K. *BAC-MP4 Heats of Formation*; Sandia National Laboratories; Livermore, CA, May, 1991.
- Saito, K.; Makishita, K.; Kakumoto, T.; Sasaki, T.; Imamura, A. *J. Phys. Chem.* **1988**, *92*, 4371.
- Lifshitz, A.; Moran, A.; Bidani, S. *Int. J. Chem. Kinet.* **1987**, *19*, 61.
- Gardiner, W. C., Jr.; Troe, J. In *Combustion Chemistry*; Gardiner, W. C., Jr., Ed.; Springer: New York, 1984; p 191.
- Stein, S. E.; Rukkers, J. M.; Brown, R. L. NIST Standard Reference Database 25, NIST Structure and Properties Database and Estimated Program, 1991.
- Stull, D. R.; Westrum, E. F., Jr.; Sinke, G. C. *The Chemical Thermodynamics of Organic Compounds*; Wiley: New York, 1969.
- Tsang, W.; Hampson, R. F. *Phys. Chem. Ref. Data* **1986**, *15*, 1087.
- Pedley, J. B.; Taylor, R. D.; Kirby, S. P. *Thermochemical Data of Organic Compounds*; Chapman and Hall: London, 1986.
- Westly, F.; Herron, J. T.; Cvetanovic, R. J.; Hampson, R. F.; Mallard, W. G. *NIST-Chemical Kinetics Data Base*, version 4.0; National Institute of Standards and Technology: Washington, D.C., 1991.
- Hoffmann, A.; Wagner, H. G.; Wolff, Th.; Hwang, S. M. *Ber. Bunsen-Ges. Phys. Chem.* **1990**, *94*, 1407.
- Frank, P.; Braun-Unkoff, M. In *Shock Tubes and Waves*, Proceedings of the 16th International Symposium on Shock Tubes and Waves, Aachen, Germany, 1987; Rheinisch-Westfälische Technische Hochschule Aachen: Aachen, Germany, 1988; p 83.
- Miller, J. A.; Bowman, C. T. *Prog. Energy Combust. Sci.* **1989**, *15*, 287.